Environ. Sci. Technol. **2003**, *37,* 569−576

Inhalation Exposure to Haloacetic Acids and Haloketones during Showering

XU XU[†] AND CLIFFORD P. WEISEL*[,†,‡]

Joint Graduate Program in Exposure Measurement & Assessment, Rutgers University and UMDNJ−Graduate School of Biomedical Sciences, and the Environmental and Occupational Health Sciences Institute, Piscataway, New Jersey 08854

Inhalation exposure to haloacetic acids (HAAs) and haloketones (HKs) in contaminated drinking water occurs during showering. The size distribution of the aerosols generated by a shower was determined using an eight size-range particle counter, which measured particles from 0.1 to >2 μm. An exponential increase in aerosol numbers was observed while the shower water was on, while the aerosol numbers declined exponentially once the water was turned off. The half-lives of the shower aerosols were longer than 5 min after the shower water was turned off. Although the majority of the shower-generated aerosols were smaller than 0.3 μm, these aerosols only contributed approximately 2% to the measured total aerosol mass. The total shower-generated particulate HAA and HK concentrations collected on an open face filter were approximately 6.3 and 0.13 μg/m^3, respectively, for shower water HAA and HK concentrations of 250 and 25 μg/L, respectively. The vapor-phase HK concentrations were 25−50 μg/m^3. The estimate of the dose from inhalation exposure of disinfection byproducts (DBPs) in the particulate phase indicate that they represent less than 1% of the ingestion dose, so inhalation is not expected to be an important exposure route to nonvolatile water contaminants or the portion of volatile DBPs that stay in the particulate phase, unless the lung is the target organ. The vapor-phase levels of volatile HKs, though, are significantly higher and can contribute greater than 10% of the ingestion dose during a shower. Thus, risk assessment to the these DBPs needs to consider the inhalation route.

1. Introduction

Inhalation exposure to water contaminants can be an important exposure route. Showering is predicted to be the major household activity resulting in inhalation exposure to volatile water contaminants (*1*). Inhalation exposure from showers occurs when water contaminants are volatilized or aerosolized and subsquently breathed. Volatile compounds are present in both the aerosol and vapor phases, while nonvolatile compounds, with small Henry's law constants, tend to remain in the aerosols.

The release of volatile organic chemicals (VOCs) from contaminated drinking water into indoor air during showering has been extensively studied (*2*−*7*) since emission of radon from drinking water into air was first recognized by Pichard and Gesell (*8*). Potential inhalation exposure to VOCs from contaminated water has also been mathematically modeled (*1*, *7*, *9*). Two approaches have been used to calculate the volatilization of VOCs, the mass-transfer coefficient (*9*), and the transfer efficiency (*5*) approaches. While the mass-transfer coefficient applies to different water-use systems, the transfer efficiency describes the volatilization of a specific compound.

Several mechanisms exist governing aerosol formation, removal, and shifts in size distribution during showering. The Pandis and Davidson's definitions of aerosols and water droplets produced during water uses are followed in this paper (*10*). A large number of large water droplets (>10 μm) and small aerosols (<10 μm) are produced from a shower spray. In addition, condensation of the water vapor in the shower air also forms small liquid aerosols. The initial size distribution of the water droplets and aerosols depends on the shower head and the water flow rate. Aerosols can be removed mainly through convection, diffusion, gravitational settling, impaction, adhesive forces, and thermophoresis (*10*−*12*). Gravitational force leads to aerosols settling onto horizontal surfaces, whereas convection and diffusion (Brownian motion) cause deposition of aerosols on surfaces of all orientations. Gravitational settling is usually the dominant process controlling the removal of larger aerosols since the settling velocity of a particle is proportional to the particle diameter squared based on Stokes's law. However, diffusion may contribute significantly to the removal of smaller aerosols (<1 μm). Thermophoresis may be an important physical phenomenon for shower aerosol removal due to the temperature changes during and after showering, while adhesion forces from surface properties and electrostatic charge might not be evident because of the high humidity in the shower stall. The small aerosol (<1 μm) population can be enhanced by droplet shattering because of the impaction of water droplets onto the walls and the floor of the shower stall. Evaporation also shifts the aerosol size distribution to a smaller size range, while coagulation of small particles forms larger aerosols and shifts the size distribution to a larger size range.

In general, aerosols less than 7 μm may reach the gas exchange (alveolar) region and, therefore, contribute significantly to inhalation exposure (*13*). Aerosols smaller than 0.1 μm undergo Brownian motion and generally grow to sizes larger than 0.1 μm through coagulation. Droplets larger than 10 μm settle quickly and can be effectively removed in the upper respiratory tract. Inhalation exposure to nonvolatile chemicals in aerosols is affected by the size distribution of aerosols, the rate of the aerosol generation (emission rate), their concentrations in water, and the removal rate of aerosols. While the size distribution of aerosols larger than 1 μm in a shower has been studied (*14*, *15*), little information has been reported for submicrometer aerosols (≤1 μm).

Epidemiological studies suggest that disinfection byproducts (DBPs) in chlorinated drinking water may be associated with bladder, rectal, and colon cancer (*16*, *17*). Trihalomethanes, haloacetic acids (HAAs), and haloketones (HKs) are the most prevalent DBPs in drinking water (*18*−*21*). Although little health information is available for brominated acetic acids, dichloroacetic and trichloroacetic acids have been classified by the U.S. EPA as group C (possible) and group B2 (probable) human carcinogens, respectively. 1,1-Dichloroproanone and 1,1,1-trichloropropanone have been shown to induce primary DNA damage in *Escherichia coli*

* Corresponding author telephone: (732)445-0154; fax: (732)445-0116; e-mail: weisel@eohsi.rutgers.edu.
† Joint Graduate Program in Exposure Measurement & Assessment.
‡ Environmental and Occupational Health Sciences Institute.

10.1021/es025747z CCC: $25.00
Published on Web 12/18/2002

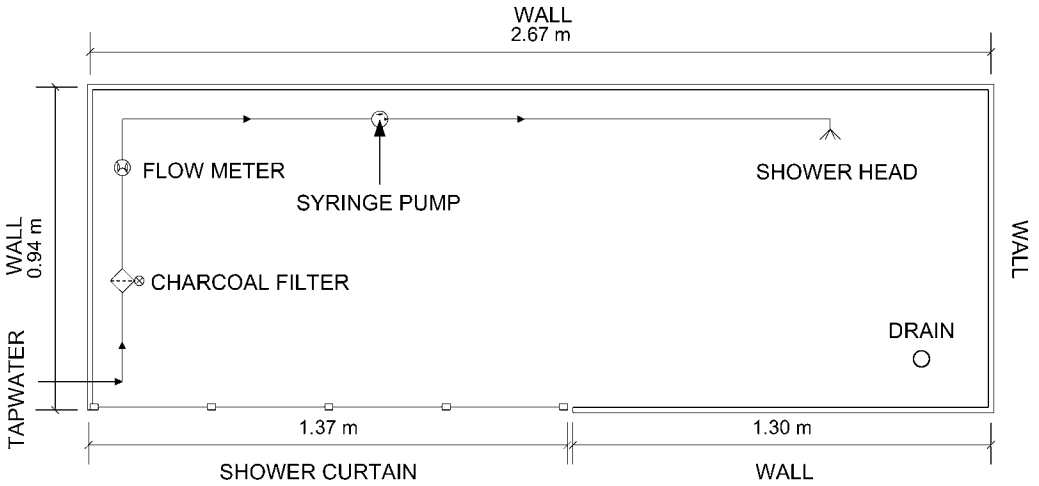

FIGURE 1. Schematic of the shower system. The charcoal filter removes DBPs from tap water; the syringe pump adds HAAs and HKs at desired concentrations; and the shower curtain covers the opening of the shower stall when shower on.

and to be mutagenic on *Salmonella typhimurium* strain TA100 (*22*). Human exposure to these compounds may cause potential adverse effects. The objectives of this study were (i) to determine the temporal emission profile and the size distribution of the aerosols (D_p: 0.1−>2 μm) produced while shower water was on; (ii) to measure the airborne particulate concentrations of 1,1-dichloropropanone, 1,1,1-trichloropropanone, chloroacetic acid, dichloroacetic acid, bromoacetic acid, trichloroacetic acid, bromochloroacetic acid, and dibromoacetic acid during a 10-min time period while shower water was on; (iii) to evaluate the transfer of semivolatile HKs from shower water to vapor phase by measuring the concentrations of the volatilized HKs in the shower air; and (iv) to assess the potential inhalation doses of the DBPs during showering.

2. Materials and Methods

2.1. Shower System. The shower stall in which the experiments were conducted had a volume of 6 m^3 with dimensions of 2.67 m (length) × 0.94 m (width) × 2.39 m (height) (Figure 1). The shower stall was located in the Environmental and Occupational Health Sciences Institue and used exclusively for the experiments. The shower experiments were conducted using a residential-type showerhead with a fine water stream setting and a water temperature between 36 and 38 °C. A shower curtain was used to separate the shower stall from the rest of the bathroom while the water was on to minimize the air exchange rate. The water flow rate of the shower varied from 7 to 10 L/min. The experiments were conducted in an unoccupied shower stall.

A charcoal filter and chemical delivery system was added to the shower system to provide the desired water DBP concentration. Tap water was passed through a granular activated carbon filter (4234372, Kenmore Water Line, Hoffman Estates, IL) to remove organic contaminants, and the desired amount of haloacetic acids or haloketones was continuously injected into the water prior to the shower head with a constant-flow syringe pump. Water HK and HAA concentrations were approximately 25 and 250 μg/L, respectively. On the basis of the Information Collection Rule (ICR) auxiliary I database (*23*), the maximum concentration of 1,1,1-trichloropropanone was determined to exceed 20 μg/L. Concentrations greater than 200 μg/L have been measured in swimming pools for a variety of DBPs (*24*). Therefore, these concentration levels may represent the maximum expected concentrations of HKs and HAAs in a poorly controlled water system or swimming pool.

2.2. Characterization of the Aerosol Size Distribution. A Lasair model 1002 optical particle counter (Particle Measuring Systems, Inc., Boulder, CO) was used to determine the size distribution of aerosols generated by the shower. The particle counter measured particles from 0.1 to greater than 2 μm in size (particle diameter), grouped into eight size ranges: 0.1−0.2, 0.2−0.3, 0.3−0.4, 0.4−0.5, 0.5−0.7, 0.7−1.0, 1.0−2.0, and >2 μm. The optical counter draws air into a small chamber at a flow rate of 0.002 cfm (57 mL/min) where the particles are sized and counted by measuring the amount of laser light scattered from each particle. The shower air was sampled through a 1.75-m stainless steel tube with the inlet placed in the breathing zone height (1.5 m) of the shower stall. The stainless steel tube resulted in negligible loss of aerosols based on a comparison of aerosol counts with and without the stainless steel tube. Aerosol losses were found in Teflon and copper tubes. Aerosol counts were monitored continuously for 42 min, starting with a 6-min background sampling period before the shower water was turned on, a 10-min shower, and a 26-min time period after the shower water was turned off. The shower curtain was kept closed while the water was on and left open when it was off.

2.3. Sampling and Analysis of Particulate DBP Concentration. Whatman Glass Microfiber Filters (Type GF/B, Fisher Scientific Inc., Pittsburgh, PA) were used to collect the aerosols generated by the shower. The filters were soaked in a NaOH solution (0.5 M) and then dried for storage. Prior to use, the filters were wetted with a spray of deionized water and then placed in open-face filter holders. The pump flow rate was set to 0.7 L/min, and the air sample was collected for 10 min while the shower water was on. The filters were located approximately 5−10 cm from the shower stream at breathing zone height. Since an open-face filter holder was used, both aerosols (<10 μm) and water droplets (>10 μm) were collected. After sampling, each filter was placed into a 15-mL centrifuge tube containing 5 mL of deionized water. To analyze HAAs, the water was acidified to pH <2 with 0.5 mL of concentrated H_2SO_4. The HAAs were extracted from the water sample using methyl *tert*-butyl ether (MTBE), methylated to their methyl esters using acidic methanol, and analyzed using GC/ECD (*25*). Haloketones collected by the filters were extracted by MTBE and analyzed by GC/ECD (*26*).

2.4. Sampling and Analysis of Gas-Phase HK Concentration. Breathing zone air samples were collected in the shower stall at a height of 1.5 m using stainless steel absorbent traps (0.5 cm i.d. × 8.8 cm, Perkin-Elmer Inc., Shelton, CT) packed with 0.25 g of Tenax TA (Supelco Inc., Bellefonte, PA). Newly packed traps were conditioned at 270 °C for 6 h with a constant flow of zero-grade nitrogen (Air and Chemicals Inc., Allentown, PA) at approximately 10 mL/min.

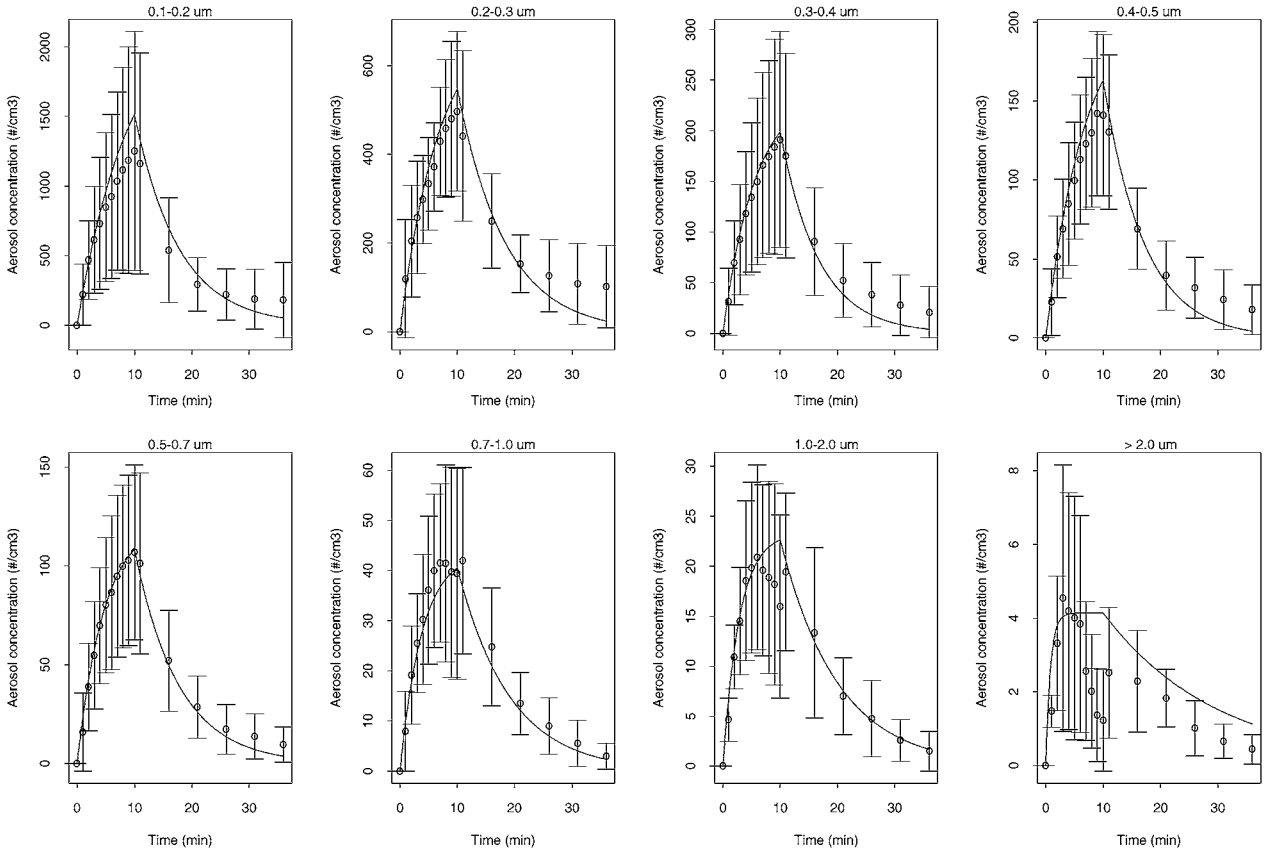

FIGURE 2. Concentration profile of aerosols in a shower stall while the shower water was on and off by particle size range. The shower water was turned on at 0 min and off at 10 min. The error bars represent the standard deviations of the observations from 10 replicate experiments ($N = 10$) at each sampling time point. (○) Mean observations; (—) one-compartment model fit.

Used sampling traps were reconditioned at 270 °C for 4 h, and the adsorbent was replaced after 10 uses. The conditioned traps were sealed with Teflon caps and stored in a plastic bag filled with zero-grade nitrogen until use. A constant flow pump (model 224-43XR, SKC Inc., Eighty Four, PA) was used to draw air through the Tenax trap. The flow rate of the pump was set to approximately 100 cm^3/min using a low flow adaptor and calibrated before and after each experiment using a DryCal primary flow meter (SKC Inc.) with a Tenax trap in the sampling train. Three replicate air samples were collected at 20 min after the shower water was turned on for 1 min. Duplicate air samples were collected before the shower was turned on to determine the background air HK concentration. After sampling, the Tenax trap was removed from the sampling train and stored in a plastic bag containing zero-grade nitrogen until analysis.

The haloketones were desorbed from the trap at 250 °C using an automated thermal desorption system (ATD-400, Perkin-Elmer Inc.) and transferred to a capillary GC (Hewlett-Packerd 5890, DB-5 capillary column, 60 m × 0.25 mm i.d., 1 μm film thickness) system equipped with an ECD detector. The target HK compounds were quantified by comparing the peak areas of the HKs in samples to external standards.

2.5. Determination of Air Exchange Rate. The air exchange rate between the shower stall and the bathroom was determined by measuring the decay of sulfur hexafluoride with a multi-gas monitor (Type 1302, INNOVA Air Tech Instruments, Denmark). The background sulfur hexafluoride concentrations were very low (approximately 0.05 ppm) in the shower stall. Sulfur hexafluoride (Scott Specialty Gases Inc, Plumsteadville, PA) was delivered into the shower stall through a Tygon tubing to provide concentrations of 1−3 ppm. After mixing the sulfur hexafluoride in the shower stall using a fan, the concentration was monitored at a breathing zone height once every 3 min for 30 min. The air exchange rate in the shower stall was measured when the shower water was on and off. Five replicate air exchange measurements were made for each water condition on different days. The air exchange rate was calculated as the slope of the regression line ($R^2 > 0.99$) of the logarithm of the sulfur hexafluoride concentration as the dependent variable and time as the independent variable.

3. Results

3.1. Emission and Removal of Aerosols. Particle number concentration is used to express the particle count (#/cm^3) in each size range (*27*). The temporal changes in particle number concentration during and after a shower are plotted in Figure 2. The background particle number concentration was measured before each shower experiment. Assuming that the background particle number concentration remained constant during the entire period of each experiment, the changes in particle number concentration would be due to shower-generated aerosols. The number concentration of aerosols increased exponentially in all eight size ranges when the shower water was on. After the shower water was turned off, the aerosol number declined exponentially. Large variability in aerosol number concentration was observed for different replicate experiments ($N = 10$). The variation may have been caused by the variations in the water flow rate, water temperature, air exchange rate in the shower stall, and position of the sampling inlet relative to shower stream, although no systematic analysis of the variables was done within this study.

A one-compartmental model (*28*) can be used to describe the temporal profile of aerosol number concentration in the shower stall, assuming complete and instantaneous mixing

in the shower stall:

$$N_i(t) = \frac{R_{e,i}}{V_{shower} k_{1,i}} (1 - e^{-k_{1,i}t}) \quad (\text{when } 0 \le t \le T) \quad (1)$$

$$N_i(t) = N_{max,i} e^{-k_{2,i}(t-T)} \quad (\text{when } t > T) \quad (2)$$

where $N_i(t)$ is the aerosol number concentration at time t for each detection size range i (#/cm^3, $i = 1, 2, \ldots, 8$); $R_{e,i}$ is the number emission rate for aerosols in size range i (#/min), which represents the various aerosol source terms including spraying, condensation of vapor, and droplet shattering, etc. (the contribution by droplet shattering due to the presence of a person is not included since no one was in the shower during the experiment); V_{shower} is the volume of the shower stall (m^3); $N_{max,i}$ is the peak aerosol concentration before the shower was turned off (#/cm^3); $k_{1,i}$ is the decay constant decribing all the aerosol removal processes (settling, diffusion, impaction, thermophoresis, evaporation, etc.) under dynamic conditions when the shower water is on (min^{-1}); $k_{2,i}$ is the decay constant decribing all the aerosol removal processes under static conditions when the shower water was turned off (min^{-1}); and t is time (min). The shower water was turned on at $t = 0$ and turned off at $t = T$. The number emission rate ($R_{e,i}$) and the composite decay constant ($k_{1,i}$) of the aerosols in each size range while the shower water was on were simultaneously estimated using a nonlinear regression fit to the data (eq 1, Gauss−Newton algorithm) in S-plus 2000 Professional, Release 3 (Mathsoft Inc., 2000). Assuming that an aerosol has a spherical shape and that the water density (ρ) is 1 g/cm^3, the mass of the aerosol is $^4/_3\pi r^3\rho$. This association was used to convert the emission rate in aerosol number (R_e, #/min) into an emission rate in water mass (R_e', μg/min). For calculation convenience, the midpoint of each size range was considered the diameter for all aerosols in that size range, and the range >2 μm assumed 10 μm as the upper cutoff diameter. The composite decay constant for each aerosol size range after the shower water was turned off ($k_{2,i}$) was calculated as the slope of the linear regression of the ln($N_i(t)$) and t (derived from eq 2). An R^2 greater than 0.95 was considered acceptable for computing the average value of $k_{2,i}$.

The one-compartment model (eqs 1 and 2) assumes a homogeneous aerosol number concentration throughout the shower stall. Any heterogeneity in the aerosol concentration may lead to errors in the parameter estimates. To account for heterogeneity arising from various surface effects and thermal gradients, a more complicated mathematical model would be needed, which is beyond the scope of this study. However, the high turbulence in the shower while in use may favor the well-mixing and homogeneity assumption.

The results of the emission rates and the composite decay constants are summarized in Tables 1 and 2. The decay constant of aerosols increased from 0.11 to 1.24 min^{-1} as the aerosol diameter increased while the shower water was on. The emission rate in aerosol number decreased as the aerosol size increased. The aerosol number emission rate in the size range of 0.1−0.2 μm was approximately 50 times greater than that of aerosols larger than 2 μm. However, the aerosol mass emission rate larger than 2 μm was more than 1000 times greater that of the smallest aerosols, since aerosol mass is a function of size cubed.

After the shower water was turned off, the half-lives of aerosols in all size ranges were approximately 5 min or greater (Table 2). Aerosols with diameters greater than 1 μm have longer half-lives than the smaller aerosols. The composite decay constants ($k_{2,i}$) for aerosols smaller than 2 μm were approximately 0.1 min^{-1}. However, aerosols larger than 2 μm had lower decay constants than the smaller aerosols ($\alpha \le 0.05$, one-way ANOVA and multiple comparison). The one-compartment model fitted curves are plotted in Figure 2 using the estimated parameters.

TABLE 1. Composite Decay Constant and Emission Rate of Aerosols while Shower Water Was On

size range (μm)	diameter[a] (D_p, μm)	N[b]	decay constant[c] (k_1, min^{-1})	no. emission rate[c] (R_e, $\times 10^7$ #/min)	mass emission rate[d] (R_e', μg/min)
0.1−0.2	0.15	8	0.11 ± 0.11	150 ± 107	2.65 ± 1.89
0.2−0.3	0.25	5	0.15 ± 0.10	63.4 ± 39.6	5.19 ± 3.24
0.3−0.4	0.35	8	0.18 ± 0.12	25.7 ± 16.1	5.78 ± 3.61
0.4−0.5	0.45	7	0.15 ± 0.08	18.9 ± 9.53	9.02 ± 4.55
0.5−0.7	0.6	9	0.21 ± 0.12	15.6 ± 9.44	17.6 ± 10.7
0.7−1.0	0.85	8	0.26 ± 0.15	6.83 ± 2.33	22.0 ± 7.50
1.0−2.0	1.5	6	0.35 ± 0.21	4.90 ± 0.72	68.9 ± 12.8
>2.0	6	4	1.24 ± 0.27	3.08 ± 0.70	3490 ± 795

[a] The midpoint of the size range. [b] Number of experiments used for the nonlinear regression calculations. [c] All parameter estimates were statistically significant at $\alpha = 0.05$. [d] $R_e' = R_e \times {}^4/_3\pi(D_p/2)^3 \times 10^{-6}$.

TABLE 2. Composite Decay Constant and Half-Life of Aerosols after Shower Water Was Turned Off

size range (μm)	N[a]	decay constant[b] (k_2, min^{-1})	half-life (min)
0.1−0.2	10	0.13 ± 0.05	5.5 ± 2.1
0.2−0.3	5	0.12 ± 0.04	5.8 ± 1.9
0.3−0.4	7	0.15 ± 0.04	4.7 ± 1.3
0.4−0.5	8	0.14 ± 0.03	5.1 ± 1.3
0.5−0.7	6	0.13 ± 0.05	5.3 ± 1.8
0.7−1.0	10	0.11 ± 0.03	6.3 ± 2.0
1.0−2.0	7	0.10 ± 0.02	8.3 ± 2.3
>2.0	6	0.05 ± 0.01	13 ± 2.7

[a] Number of experiments used to calculate the linear regression. [b] $R^2 \ge 0.95$ for each linear fit.

3.2. Size Distribution of Aerosols. The aerosol size distribution at the end of the shower is plotted in Figure 3 as the normalized count distribution: $\Delta N/\Delta \log D$ versus log D, where ΔN is the number concentration of aerosols within the diameter interval whose midpoint was D (*29*). The majority of the shower-generated aerosols were in the smallest two size fraction ranges (0.1−0.2 and 0.2−0.3 μm). As the diameter of aerosols increased, the normalized number of aerosols in a given size range decreased. The aerosol number concentration in the smallest size range, 0.1−0.2 μm, was several orders of magnitude higher than the number concentration of the aerosols with a diameter greater than 2 μm (Table 3). The mass distribution of the aerosols in each size range was calculated assuming spherical-shaped aerosol with a density of 1 g/cm^3 (Table 3). The contribution of the smallest aerosols (<0.3 μm) to total aerosol mass was considerably less than the mass from the largest aerosols (90% for aerosols >1.0 μm).

3.3. Total Particulate Concentrations of HAAs and HKs. Since the open-face sampling inlet does not discriminate against water droplets (>10 μm), the mass collected during the showers represents the total mass of the aerosols and water droplets in the shower air. The breathing zone particulate HAA concentrations ranged from 3.88 to 9.98 μg/m^3 while the 1,1-dichloropropanone and 1,1,1-trichloropropanone particulate concentrations associated with the shower-derived aerosols and droplets were 0.185 and 0.071 μg/m^3, respectively (Table 4).

3.4. Air Exchange Rate in the Shower Stall. The air exchange rates (k_{air}) while the shower water was on and off were 0.14 ± 0.027 and 0.058 ± 0.023 min^{-1} ($N = 5$), respectively. Thus, when the shower was on, the air exchange

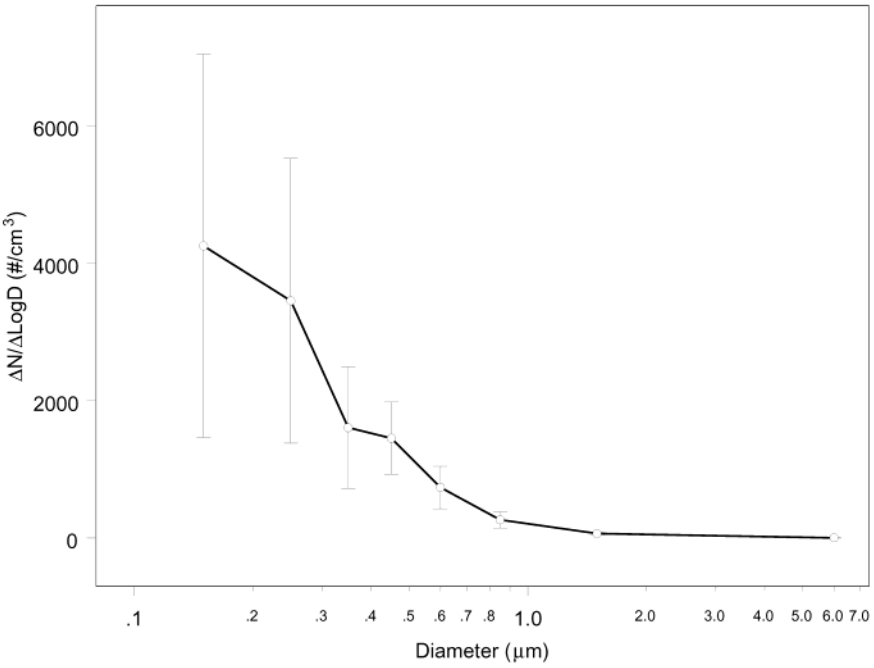

FIGURE 3. Particle size distribution just prior to the end of the shower ($t = 10$ min) using the average diameter to represent the size range.

TABLE 3. Characterization of Peak Aerosol Number and Mass Just Prior to the End of the Shower ($t \simeq 10$ min)

range of size (μm)	diameter[a] (μm)	particle number ($\pm$SD, #/cm^3)	particle mass ($\pm$SD, μg/m^3)
0.1−0.2	0.15	1280 ± 837	2.3 ± 1.5
0.2−0.3	0.25	622 ± 373	5.1 ± 3.1
0.3−0.4	0.35	193 ± 106	4.3 ± 2.4
0.4−0.5	0.45	141 ± 51	6.7 ± 2.4
0.5−0.7	0.60	108 ± 45	12.2 ± 5.1
0.7−1.0	0.85	43 ± 19	13.8 ± 6.1
1.0−2.0	1.5	20 ± 8	35.3 ± 14.1
>2.0	6.0	3 ± 2	339 ± 226
total		1780 ± 1070	414 ± 258

[a] The midpoint of the size range.

TABLE 4. Total Particulate Concentrations of HAAs and HKs in the Shower Stall

compound	N[a]	water concn (μg/L)	PM DBP concn[b] (μg/m^3)
1,1-dichloropropanone	8	24.9 ± 1.62	0.185 ± 0.049
1,1,1-trichloropropanone	8	25.3 ± 1.14	0.071 ± 0.031
chloroacetic acid	7	257 ± 11.3	9.98 ± 4.58
bromoacetic acid	7	270 ± 6.71	8.47 ± 3.19
dichloroacetic acid	7	280 ± 47.2	6.64 ± 2.58
trichloroacetic acid	7	300 ± 78.2	4.47 ± 2.30
bromochloroacetic acid	7	238 ± 72.4	4.25 ± 1.95
dibromoacetic acid	7	249 ± 97.5	3.88 ± 2.30

[a] The number of replicate experiments conducted. [b] The measured total PM concentrations of the DBPs.

rate in the shower stall was approximately twice that when the shower water was off.

3.5. Vapor-Phase HKs. A significant portion of the HKs is expected to evaporate into the vapor phase, based on their relatively high Henry's law constants. Five shower experiments were conducted to determine the vapor-phase HK concentrations. The average 1,1-dichloropropanone concentrations in the air between 20 and 21 min after the start of the shower varied from 41.1 to 54.0 μg/m^3 for a water concentration range from 24.1 to 29.6 μg/L. The average 1,1,1-trichloropropanone concentrations in the air during the same time period were from 24.9 to 44.7 μg/m^3 for a water concentration range from 25.6 to 31.5 μg/L.

There were two ventilation fans located in the ceiling of the adjacent bathroom, and the air exchange rate between the bathroom and the rest of the building was approximately 2 times greater than the air exchange rate between the shower stall and the bathroom. Therefore, it is not likely that the chemicals would accumulate in the bathroom air over the experiment period, and a single-compartment plug flow stream model has been used to describe emissions of volatile compounds, such as HKs, from a shower (*9*, *30*). This model treats the shower as a completely mixed vessel, with an inflow and outflow air exchange with the bathroom. Assuming a zero initial air HK concentration in the shower stall, a transient mass-balance on the HK in the gas phase can be expressed as

$$V_{\text{shower}}\frac{\mathrm{d}C_{\text{air}}(t)}{\mathrm{d}t} = Q_{\text{wat}}p_{\text{vap}}C_{\text{wat}} - k_{\text{air}}V_{\text{shower}}C_{\text{air}}(t) \quad (3)$$

where V_{shower} is the volume of the shower (m^3); Q_{wat} is the shower water flow rate (L/min); p_{vap} is the weight fraction volatilized from the shower water (or transfer efficiency); k_{air} is the shower air exchange rate (min^{-1}); C_{wat} (μg/L) is the HK concentration in shower water; and $C_{\text{air}}(t)$ is the HK concentration in the air within the shower stall at time t (μg/m^3). The air HK concentration ($C_{\text{air}}(t)$) can be solved, assuming $C_{\text{air}}|_{(t=0)} = 0$, by

$$C_{\text{air}}(t) = \frac{Q_{\text{wat}}p_{\text{vap}}C_{\text{wat}}}{k_{\text{air}}V_{\text{shower}}}[1 - \exp(-k_{\text{air}}t)] \quad (4)$$

Given the time-averaged HK concentrations in the vapor phase, the transfer efficiency (p_{vap}) was solved by integrating eq 4. The average transfer efficiency of DCP and TCP were 0.17 ± 0.086 and 0.11 ± 0.091, respectively. The emission rate was calculated as $Q_{\text{wat}}C_{\text{wat}}p_{\text{vap}}$. The emission rate of DCP was 40.6 ± 20.3 μg/min, and the emission rate of TCP was 27.8 ± 23.9 μg/min (Table 5). It can be also noted that based

TABLE 5. Calculation of Transfer Efficiency and Emission Rates of HKs

expt	water concn[a] (μg/L, $n = 4$)	water flow (L/min)	air concn[b] (μg/m^3, $n = 3$)	transfer efficiency (%)	emission rate (μg/min)
			1,1-Dichloropropanone		
I	28.4 ± 2.3	8.7	49.0 ± 10.1	17 ± 3.4	41.8 ± 8.6
II	29.6 ± 3.6	7.8	54.0 ± 19.1	20 ± 7	46.0 ± 16.2
III	24.1 ± 1.9	9.2	47.9 ± 0.9	18 ± 0.44	40.8 ± 0.8
IV	27.7 ± 3.2	9.5	41.1 ± 6.4	13 ± 2.1	35.0 ± 5.4
V	25.8 ± 2.6	9.1	46.4 ± 8.1	17 ± 3	39.6 ± 6.9
overall	27.1 ± 6.2	8.9 ± 0.7	47.8 ± 23.9	17 ± 8.6	40.6 ± 20.3
			1,1,1-Trichloropropanone		
I	27.8 ± 3.4	8.7	42.1 ± 7.7	15 ± 2.7	35.9 ± 6.5
II	31.5 ± 4.3	7.8	44.7 ± 22.1	15 ± 7.6	38.1 ± 18.9
III	25.6 ± 2.1	9.2	25.6 ± 0.5	9.3 ± 0.32	21.8 ± 0.4
IV	29.2 ± 3.0	9.5	24.9 ± 12.5	7.7 ± 3.9	21.2 ± 10.6
V	27.8 ± 2.4	9.1	25.9 ± 9.1	8.8 ± 3.1	22.0 ± 7.8
overall	28.4 ± 10.0	8.9 ± 0.7	32.6 ± 28.1	11.1 ± 9.1	27.8 ± 23.9

[a] Water samples were collected at 5, 10, 20, and 30 min after shower water was turned on. [b] Three replicated air samples were collected.

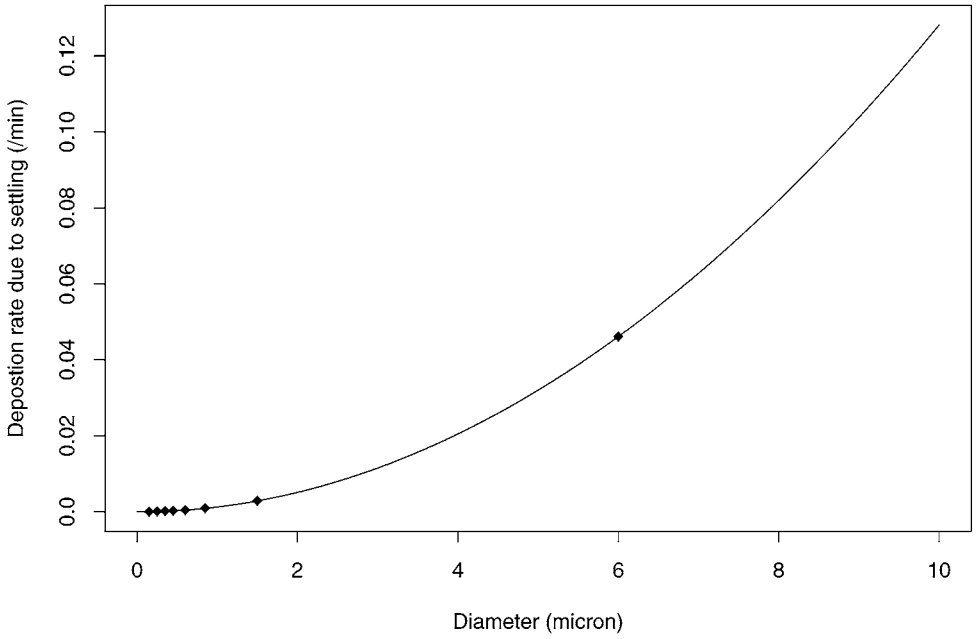

FIGURE 4. Deposition rate of particles: calculated from Stokes's law, and slip correction factors are applied to the particles smaller than 1 μm. The deposition height is assumed to be 1.5 m.

on the measured air exchange rate while the shower was on, the vapor-phase HK concentrations would approach a steady state after 20 min, the time when the sampling started.

4, Discussion

4.1. Removal Processes of Aerosols in the Shower Stall. Gravitational settling is an important physical process controlling the removal of larger aerosols and water droplets. The deposition rate due to settling was calculated according to Stokes's law (Figure 4) assuming a deposition height of 1.5 m. Slip correction factors were applied to aerosols smaller than 1.0 μm. The aerosols smaller than 2 μm do not have a significant settling rate, while the deposition rate due to settling for a 6-μm aerosol is approximately 0.05 min^{-1}.

The removal of small aerosols is usually dominated by diffusion and convection related to air exchange (*12*, *31*). To evaluate whether convection was controlling the aerosol removal, the average aerosol decay constant in each size range while the shower water was on (Table 1) and off (Table 2) was compared to the average air exchange rate during the two time periods using a two-sample *t* test. The *P* values are summarized in Table 6. While the shower water was on, the composite decay constants for aerosols smaller than 2 μm were not statistically different from the air exchange rate. Thus, their removal appears to be controlled by movement of air in to and out of the shower suggesting that diffusion

TABLE 6. Comparison of Particle Removal Rate to Air Exchange Rate[a]

range of size	*P* value (p_1)[b]	*P* value (p_2)[c]
0.1−0.2	0.58	0.01
0.2−0.3	0.82	0.01
0.3−0.4	0.47	<0.01
0.4−0.5	0.78	<0.01
0.5−0.7	0.22	0.02
0.7−1.0	0.11	<0.01
1.0−2.0	0.07	0.11
>2.0	<0.01	0.37

[a] Two-sample *t* test. [b] *P* value for comparison of decay constant to air exchange rate when shower water was on. [c] *P* value for comparison of decay constant to air exchange rate when shower water was off.

and convection are the dominant processes for the removal of the smallest aerosols during the high-turbulence and dynamic period. The composite decay constant for the aerosols larger than 2 μm was much greater than the sum of the deposition rate due to settling and the air exchange rate during this period, indicating that the other depostion processes (e.g., thermophoresis) played an important role for removal of the larger aerosols as well. However, a different phenomenon was observed for the removal of aerosols once the shower water was turned off. The smallest aerosols (D_p < 1 μm) had much greater composite decay constants than the air exchange rate. One process that might contribute significantly to the removal of the small aerosols in the shower stall after the shower water was turned off is evaporation. Pandis and Davidson (*10*) have mathematically modeled evaporation of water droplets and identified that smaller water droplets evaporated faster. They also showed that evaporation increased as humidity decreased. The humidity of the shower stall is expected to decrease after the shower water is turned off. The post-shower decay constant calculated for > 2 μm (Table 2) was similar to the settling rate for a 6-μm aerosol. However, since the calculated decay constant is actually the net difference between losses and production, the composite decay constant of these aerosols may result from the combination of gravitational settling, thermophoresis, evaporation, and coagulation of small aerosols forming larger aerosols.

4.2. Estimating Respirable Particulate DBP Concentrations. The time-averaged concentrations of the DBPs in the respirable aerosols ($C_{aerosol}$, ng/m^3) can be estimated assuming (i) no partitioning of the chemicals from shower water to air occurs during the aerosol generation process; (ii) unit density for water; (iii) the midpoint of the size range represents the size of all the aerosol in that size range; and (iv) the aerosols, prior to evaporation have the same DBP concentration as the shower water; from the following:

$$C_{aerosol} = \frac{\sum_{i=1}^{m} \int_0^{t_{exp}} C_i(t)\, dt}{\rho t_{exp}} \times 10^{-6} \times C_{wat} \quad (5)$$

$$C_i(t) = \frac{4}{3}\pi (D_p/2)^3 \rho N_i(t) \quad (6)$$

where C_{wat} is the DBP concentration in shower water (μg/L); m is the number of particle size ranges (m = 8); t_{exp} is the shower duration (10 min); $C_i(t)$ is the aerosol mass concentration for size range i at time t (μg of H_2O/m^3); $N_i(t)$ is the aerosol number concentration for size range i at time t (eq 1, #/m^3); and ρ is water density (1 g/cm^3). On the basis of the calculations, the DBPs in shower water at 1 μg/L would produce a DBP airborne concentration of 0.0005 ng/m^3 in the respirable aerosols during the 10-min shower. Therefore, the estimated respirable particulate-phase HAA and HK concentrations were approximately 0.13 and 0.01 ng/m^3, assuming no partitioning of HKs, respectively, arising from concentrations in water of 250 μg/L for HAAs and 25 μg/L for HKs.

On the basis of a size distribution characterized by Keating and McKone (*15*), the airborne concentration of a nonvolatile compound in respirable particles would be 0.004 ng/m^3 during showering when the chemical concentration in the shower water is 1 μg/L (*13*). As described by Pandis and Davidson (*10*), Gunderson and Witham determined that for a shower water concentration of 1 μg/L the respirable particulate (<10 μm) concentration of ammonium fluorescein, a nonvolatile compound, would be 0.03−0.2 ng/m^3 within a shower stall. Finley et al. obtained similar results based on their shower studies on Cr(VI) contaminated water (*32*), although the size of the collected aerosols was unclear. The measured concentrations of the nonvolatile compounds in the respirable particulate phase were 1 or 2 orders of magnitude higher than the estimates based on the aerosol size distributions. The use of a mannequin in Finley et al.'s and Gunderson and Witham's shower studies may have enhanced the shattering of water droplets and the formation of smaller aerosols. Differences are also expected because of variations in water spray, which alters the aerosol size distribution and amount of aerosol produced, size of shower stall, location of the sampler in the stalls, air exchange rate, water evaporation rate, etc.

TABLE 7. Parameters of the Hypothetical Shower Exposure Scenario

parameter	value
inhalation rate (R_{inh})[a]	20 m^3/day
shower duration (t_{exp})	10 min
water flow rate (Q_{wat})	10 L/min
shower volume (V_{shower})	2 m^3
air exchange rate (k_{air})[b]	1.26 ACH
shower frequency (λ) [a]	0.74 shower/day
water temperature	38 °C

[a] U.S. EPA, 1997 (*31*). [b] Since a higher air exchange rate was found during showering, the 90th percentile value was selected from Table 17-10 in ref *31*.

TABLE 8. Comparison of Potential Daily DBP Inhalation Dose during the Hypothetical Shower Exposure with the Daily DBP Ingestion Dose

compound	C_{wat}[a]	D_{ing}[b]	$D_{aerosol}$ (%)[c]	D_{vap} (%)[d,e]
1,1-dichloropropanone	24.9	34.9	0.019 (0.055)	10.2 (29.3)
1,1,1-trichloropropanone	25.3	35.4	0.007 (0.021)	6.7 (18.9)
chloroacetic acid	257	360	1.03 (0.29)	–
bromoacetic acid	270	378	0.88 (0.23)	–
dichloroacetic acid	280	392	0.69 (0.18)	–
trichloroacetic acid	300	420	0.46 (0.11)	–
bromochloroacetic acid	238	333	0.44 (0.13)	–
dibromoacetic acid	249	349	0.40 (0.12)	–

[a] Shower water DBP concentration (μg/L): upper limits for poorly controlled water systems. [b] Daily DBP ingestion dose based on a water ingestion rate of 1.4 L/day (μg/day). [c] Daily inhalation dose of aerosolized DBP from shower exposure (μg/day). [d] Daily inhalation dose of vaporized DBP from shower exposure (μg/day). [e] Assume no vaporized HAAs in the shower air.

4.3. Estimating Potential Inhalation Doses of the DBPs. The daily potential inhalation doses of particulate HKs and HAAs and vapor-phase HKs generated during showering were calculated for an adult. The experimental DBP water concentrations listed in Table 4 were used for estimating the potential doses. A hypothetical exposure scenario is assumed and described in Table 7 for the dose estimation. A typical residential shower volume (2 μm^3) was chosen to calculate the doses during the hypothetical exposure rather than the shower volume used in the experiments. The daily ingestion dose of each individual DBP was also estimated for comparison based on a tap water ingestion rate of 1.4 L/day (*31*) (Table 8).

Assuming the worst case scenario where 100% of the inhaled aerosols are deposited in the lung of a person, the daily dose of exposure to DBP aerosols ($D_{aerosol}$, μg/day) from a shower is calculated as follows:

$$D_{aerosol} = \lambda t_{exp} C_a R_{inh} \quad (7)$$

where λ is the shower frequency; t_{exp} is the shower duration; R_{inh} is the inhalation rate; and C_a is the particulate DBP concentration (μg/m^3).

Although the cutoff size of 10 μm is usually chosen to represent the upper limit of the "inhalable particulates",

Pandis and Davidson (*10*) indicated that water droplets between 10 and 50 μm should not be neglected for the exposure estimates in a shower since once the droplets leave the area of 100% relative humidity they begin to evaporate, producing respirable aerosols that will have higher concentrations of the nonvolatile solutes. To date, little information has been reported for shower-generated water droplets in the size range from 10 to 50 μm. The total PM DBP concentrations (Table 4) measured in this study may represent upper-bound exposure concentrations for the shower conditions and include water droplets larger than 10 μm. Therefore, the average measured values were used to estimate the DBP doses from inhalation exposure during showering. It was assumed that the PM DBP concentrations (C_a) remained constant (uniformly distributed) during the 10-min shower. Subsquent exposures to aerosols in the bathroom or other sections of the house is beyond the scope of the current manuscript. The size distribution data presented can be used to model the dispersion of the aerosols throughout the residential microenvironment.

The potential daily dose of vaporized HKs (D_{vap}, μg/day) from the shower is calculated by the following equation:

$$D_{vap} = \lambda R_{inh} \int_0^{t_{exp}} C_{air}(t)\, dt \qquad (8)$$

where $C_{air}(t)$ is calculated by eq 4 based on the estimated average p_{vap} values for the HKs (Table 5).

Haloacetic acids are expected to be completely ionized in tap water at a pH close to 7 and therefore are nonvolatile at ambient and typical shower water temperatures. Thus, inhalation exposure to HAAs during showering will occur predominantly through respiratory uptake of shower-generated aerosols. The average daily dose of particulate HAA calculated for showering was approximately 0.4−1.0 μg/day when the HAA concentration in water is approximately 250 μg/L (Table 8). The inhalation dose of each HAA was much lower than the corresponding daily average ingestion dose of the compound (less than 0.5%), which indicates that the potential inhalation exposure to particulate HAAs during showering is not expected to contribute significantly to the total exposure. However, shower-generated airborne HAAs will also increase the air HAA concentration throughout the home since dry HAA particles will remain in the air after the water evaporates from the aerosol. This additional exposure was not considered in the current assessment.

The daily doses of particulate HKs were also an insignificant fraction of their daily ingestion doses. However, the daily inhalation doses of vaporized DCP and TCP during showering were found to be 10.2 and 6.7 μg/day, respectively, which represent 29% and 19% of the ingestion dose, respectively. Additional inhalation exposure to HKs will also occur after an individual leaves the shower stall. It is therefore important to consider inhalation exposure to HKs when estimating their risk in drinking water.

Acknowledgments

This research was funded by the United States Environmental Protection Agency (U.S. EPA) Research Foundation (GR82-5953-01-0). This presentation has not been subjected to the Agency's review and therefore does not necessarily reflect the views of the Agency. C.P.W. is supported in part by the NIEHS Center for Excellence Grant (ES05022-06). We thank Drs. Panos Georgopoulos, Jeffrey Laskin, and Paul Lioy for reviewing the manuscript.

Literature Cited

(1) Wilkes, C.; Small, M.; Andelman, J.; Giardino, N.; Marshall, J. *Atmos. Environ.* **1992**, *26A*, 2227.
(2) Andelman, J. B. *Environ. Health Perspect.* **1985**, *62*, 313.
(3) Andelman, J. B. *Sci. Total Environ.* **1985**, *47*, 443.
(4) Andelman, J. B. In *Significance and Treatment of Volatile Organic Compounds in Water Supplies*; Ram, N., Christman, R., and Cantor, K. Eds.; Lewis Publishers: Chelsea, MI, 1990; pp 485−504.
(5) Giardino, N. J.; Andelman, J. B. *J. Exposure Anal. Environ. Epidemiol.* **1996**, *6*, 413.
(6) Jo, W. K.; Weisel, C. P.; Lioy, P. J. *Risk Anal.* **1990**, *10*, 575.
(7) McKone, T. E. *Environ. Sci. Technol.* **1987**, *21*, 1194.
(8) Pichard, H. M.; Gesell, T. F. *Health Phys.* **1981**, *41*, 599.
(9) Little, J. C. *Environ. Sci. Technol.* **1992**, *26*, 1341.
(10) Pandis, S. N.; Davidson, C. In *Exposure to Contaminants in Drinking Water*; Olin, S. S., Ed.; International Life Science Institute: Washington, DC, 1999; pp 101−110.
(11) Nazaroff, W. W.; Ligocki, M. P.; Ma, T.; Cass, G. R. *Aerosol Sci. Technol.* **1990**, *13*, 332.
(12) Owen, M. K.; Ensor, D. S.; Sparks, L. E. *Atmos. Environ.* **1992**, *26A* (12), 2149.
(13) Wilkes, C. R. In *Exposure to Contaminants in Drinking Water*; Olin, S. S., Ed.; International Life Science Institute: Washington, DC, 1999; pp 183−224.
(14) Giardino, N. J.; Esmen, N. A.; Andelman, J. B. *Environ. Sci. Technol.* **1992**, *26*, 1602.
(15) Keating, G. A.; McKone, T. E. In *Modeling of Indoor Air Quality and Exposure*; ASTM STP 1205; Nagda, N. L., Ed.; American Society for Testing Materials: Philadelphia, PA, 1993; pp 14−24.
(16) Cantor, K. P.; Lynch, C. F.; Hildesheim, M. E.; Dosemeci, M.; Lubin, J.; Alavanja, M.; Craun, G. *Epidemiology* **1998**, *9* (1), 21.
(17) Hildesheim, M. E.; Cantor, K. P.; Lynch, C. F.; Dosemeci, M.; Lubin, J.; Alavanja, M.; Craun, G. *Epidemiology* **1998**, *9* (1), 29.
(18) Christman, R. F.; Norwood, D. L.; Millington, D. S.; Johnson, J. D. *Environ. Sci. Technol.* **1983**, *17* (10), 625.
(19) Krasner, S. W.; McGuire, M. J.; Jacongelo, J. G.; Patania, N. L.; Reagan, K. M.; Aieta, E. M. *J. Am. Water Works Assoc.* **1989**, *81* (8), 41.
(20) Quimby, B. D.; Delaney, M. F.; Uden, P. C.; Barnes, R. M. *Anal. Chem.* **1980**, *52*, 259.
(21) Stevens, A. A.; Moore, L. A.; Slocum, C. J.; Smith, B. L.; Seeger, D. R.; Ireland, J. C. In *Water Chlorination: Environmental Impact and Health Effects*; Jolley, R. L., et al., Eds.; Lewis Publishers: Chelsea, MI, 1987; pp 579−604.
(22) Curieux, F.; Marzin, D.; Erb, F. *Mut. Res.* **1994**, *341*, 1.
(23) U.S. Environmental Protection Agency. *Information Collection Rule*; Federal Regulation 61:94:24354; Cincinnati, OH, 1996.
(24) Clemens, M.; Scholer, H. F. *Zentralbl. Hyg. Umweltmed.* **1992**, *193* (1), 91.
(25) Kim, H.; Weisel, C. P. *J. Exposure Anal. Environ. Epidemiol.* **1998**, *8* (4), 30.
(26) Xu, X.; Mariano, T.; Laskin, J. D.; Weisel, C. P. *Toxicol. Appl. Pharmacol.* **2002**, *184*, 19.
(27) Hinds, W. C. *Aerosol Technology: Properties, Behavior, and Measurement of Airborne Particles*; Wiley: New York, 1982; p 9.
(28) Fan, C.; Zhang, J. *Atmos. Environ.* **2000**, *35*, 1281.
(29) Finlayson-Pitts, B. J.; Pitts Jr., J. N. *Atmospheric Chemistry: Fundamentals and Experimental Techniques*; Wiley: New York, 1986; p 730.
(30) Chinery, R. L.; Gleason, A. K. *Risk Anal.* **1993**, *13* (1), 51.
(31) U.S. Environmental Protection Agency. *Exposure Factors Handbook*; EPA/600/P-95/002Fa; U.S. EPA, Office of Research and Development: Washington, DC, 1997.
(32) Finley, B. L.; Kerger, B. D.; Dodge, D. G. *J. Exposure Anal. Environ. Epidemiol.* **1996**, *6*, 229.

Received for review April 25, 2002. Revised manuscript received November 5, 2002. Accepted November 7, 2002.

ES025747Z